Phys Chem Minerals (2003) 30: 536–545
DOI 10.1007/s00269-003-0358-7
© Springer-Verlag 2003

ORIGINAL PAPER

A. M. Walker · K. Wright · B. Slater

A computational study of oxygen diffusion in olivine

Received: 10 January 2003 / Accepted: 1 August 2003

Abstract Atomistic modelling techniques are used to study the rate-determining steps that limit diffusion of oxygen in forsterite. The activation energies for diffusion parallel to all three crystallographic axes by the vacancy and interstitial mechanisms are calculated. The activation energy for extrinsic vacancy diffusion is predicted to be isotropic with a barrier height of 119 kJ mol^{-1}. Conversely, in the interstitial case it is found to be anisotropic, with extrinsic activation energies that range between 94 and 178 kJ mol^{-1}. The effect of intrinsic defects and two typical impurities, iron and hydrogen, upon diffusion is also considered. We find that the migration energy is slightly higher in iron-rich fayalite compared with forsterite and that the presence of hydrogen defects will not affect the diffusion mechanism. These observations lead us to reinterpret existing experimental results on oxygen diffusion in natural olivine. We suggest that at low oxygen partial pressure the mechanism observed is a vacancy mechanism, while at high oxygen partial pressure the mechanism is interstitial. We believe that this change in mechanism is mediated by iron redox reactions. Taking this process into account, we derive activation energies in excellent agreement with those found experimentally in natural samples of olivine. The anisotropy of activation barriers and hence the change in diffusion rates with temperature could be used to distinguish between the two mechanisms in future experimental work.

Keywords Oxygen · Diffusion · Olivine · Forsterite

A. M. Walker (✉) · K. Wright · B. Slater
Davy Faraday Research Laboratory,
The Royal Institution of Great Britain,
21 Albemarle Street,
London, W1S 4BS, UK
e-mail: andreww@ri.ac.uk
Tel.: +44 0-20-7409-2992
Fax: +44 0-20-7629-3569

A. M. Walker · K. Wright
Department of Earth Sciences,
University College London,
Gower Street,
London, WC1E 6BT, UK

K. Wright
Department of Chemistry,
Christopher Ingold Laboratories,
University College London,
20 Gordon Street,
London, WC1H 0AJ, UK

Introduction

The mineral olivine forms a solid solution with composition ranging between Mg_2SiO_4 (forsterite, Fo_{100}) and Fe_2SiO_4 (fayalite, Fo_0). With composition $Fo_{\approx 90}$, olivine forms 60% of the Earth's upper mantle, making it one of the most abundant minerals on Earth. Therefore, the self-diffusion of the components of olivine will have a major influence on many geophysical phenomena; for example, diffusion will affect the rheology and electrical conductivity of the mantle and the growth rate of new phases as mantle material passes into the transition zone. Consequently, establishing the diffusion coefficients of olivine's major constituents as a function of temperature, pressure and chemistry are of great interest to the geophysicist. The diffusion of oxygen is no exception as it plays a role in controlling mantle rheology and the growth rate of new phases. In this context oxygen diffusion has been measured in both synthetic forsterite (Sockel and Hallwig 1977; Jaoul et al. 1980, 1983; Reddy et al. 1980; Sockel et al. 1980; Ando et al. 1981; Oishi and Ando 1984) and in natural olivine samples (Houlier et al. 1988; Gérard and Jaoul 1989; Ryerson et al. 1989; Dohmen et al. 2002). Despite these quantitative experimental data, on the atomic scale the oxygen diffusion mechanism remains unknown. This paper aims to characterize the underlying mechanism by using computational modelling techniques. These methods are able to provide qualitative and quantitative insights into atomistic mechanisms that control diffusion in natural and synthetic samples.

Structurally, olivine can be described as either an isosilicate or a hexagonally close-packed (HCP) lattice of oxygen ions with half of the octahedral sites occupied by iron or magnesium ions and one eighth of the tetrahedral sites occupied by silicon ions. These ions distort the HCP lattice and give olivine orthorhombic symmetry (throughout this paper the space group setting *Pbnm* is used; however, no symmetry is applied to constrain the calculations). The olivine unit cell, shown in Fig. 1, contains three symmetry-inequivalent oxygen sites (O1, O2 and O3), two metal sites (M1 and M2) and one silicon site. Two unoccupied octahedral sites (I1 and I2) are related to M1 and M2. I1 and M1 are on inversion centres and I2 and M2 lie on a mirror plane.

Diffusion coefficients show an Arrhenius behaviour, where the diffusion coefficient, D, at temperature T is described by Eq. (1).

$$D = D_0 \exp\left[-\frac{E}{RT}\right] \quad , \tag{1}$$

where R is the gas constant, E is an activation energy and D_0 is the pre-exponential factor which depends on other factors that control diffusion rate (for example the vibrational frequency of the diffusing ion and the hop length between adjacent sites in the lattice). The activation energy for oxygen diffusion has been measured in synthetic forsterite by Jaoul et al. (1980, 1983) (320 and 293 kJ mol^{-1} respectively), Reddy et al. (1980) (372 kJ mol^{-1}) and Ando and co-workers (Ando et al. 1981; Oishi and Ando 1984) (415 kJ mol^{-1}). In natural olivine, the activation energy has been measured in samples of San Carlos olivine by Gérard and Jaoul (1989) (318 kJ mol^{-1} parallel to [001]) and Ryerson et al. (1989) (266 kJ mol^{-1} parallel to [100]). More recently, the diffusion has been measured in olivine of mantle origin by Dohmen et al. (2002), this study yields an activation energy of 338 kJ mol^{-1} parallel to [001]. These measurements utilize natural samples with approximate composition Fo_{90}. There are no data available on oxygen diffusion in olivines with other compositions.

For synthetic forsterite, there is compelling experimental evidence that the activation energy for oxygen diffusion is isotropic; both Reddy et al. (1980) and Jaoul et al. (1983) measured diffusion in all three directions and did not observe a difference in activation energy. However, the diffusion rate has been observed to be fastest along the [010] direction (Reddy et al. 1980). Intriguingly, as the activation energy is equal in each direction, the anisotropy of the diffusion coefficient must be an expression of an underlying inequivalence of the pre-exponential factor for diffusion.

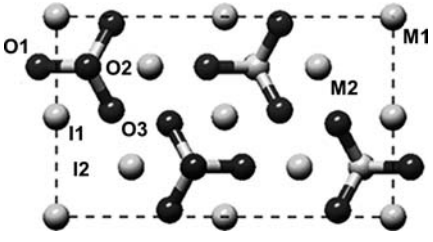

Fig. 1 The olivine unit cell looking along [100] with oxygen in *dark grey*, magnesium in *mid-grey* and silicon in *light grey*, shown bonded to the oxygen. The oxygen atoms *O1* and *O2*, silicon and magnesium *M2* lie on the mirror plane, magnesium *M1* is on an inversion centre and oxygen *O3* is in a general position. The two interstitial positions *I1* (obscured by magnesium M1 ions in this view) and *I2* are also indicated

In natural olivine the activation energy has been reported only for diffusion parallel to the [100] and [001] axes. However, some data are available for diffusion parallel to [010] in natural olivine, summarized in Fig. 14 of Ryerson et al. (1989). At low oxygen partial pressures (with a Fe–FeO oxygen buffer) this figure shows that the variation in diffusion rate with temperature appears to be isotropic, but at high oxygen partial pressure (Ni–NiO buffer) the apparent activation energy parallel to [010] is 71 kJ mol^{-1} higher than parallel to [100]. It is in this context that our investigation is particularly relevant, since we can explore atomic transport directly and with relation to one axis, or indeed any combination of axes.

As well as being temperature-dependent, the diffusion coefficient also varies with the concentration of the defects that permit diffusion. This can provide a powerful method to deduce the diffusion mechanism, if the concentration of the diffusing defects can be varied in a controlled way by, for example, altering the chemistry of the sample's surroundings. In olivine, the variation in the concentration of point defects with oxygen and enstatite activity has been theoretically studied by Stocker and Smyth (1977). This study has been used as a basis for the analysis of diffusion data collected with differing oxygen partial pressures. Analysis of these data is carried out by performing multivariate least-squares regression onto Eq. 1 with D_0 defined by Eq. 2.

$$D_0 = C_0 f_{O_2}^{p} \quad . \tag{2}$$

The oxygen fugacity f_{O_2} is known from the experiment, C_0, and p, are assumed to be constants found by the regression, p describes the variation of diffusion rate with oxygen partial pressure and C_0 includes all the other factors contained within D_0. With luck, p can be used to determine the nature of the diffusing species (Stocker and Smyth 1977). To simplify the argument, on an increase of the oxygen partial pressure the concentration of oxygen vacancies would be expected to drop and the concentration of oxygen interstitial ions would be expected to rise. If a vacancy mechanism operates, then the decrease in vacancy concentration with increasing oxygen partial pressure would lead to a decrease in the value of D. Conversely, if an interstitial mechanism operates, then the opposite would be true. To use this argument effectively, the charge neutrality condition (balance of charged defects in the crystal), which can be found from a knowledge of the majority point-defect type, must be known (Stocker and Smyth 1977). p has been found to be 0 in synthetic forsterite

(Jaoul et al. 1983) and approximately 0.3 in natural olivine (Gérard and Jaoul 1989; Ryerson et al. 1989). It is this positive, non-zero value of p in natural olivine that has been used to suggest that oxygen diffusion operates by the interstitial mechanism.

Although, on simple geometrical and space-filling grounds, in any close-packed oxide oxygen would be expected to diffuse by a vacancy mechanism, the experimental information has been used to argue that other mechanisms are important. For $Fo_{100,}$ oxygen diffusion is independent of oxygen partial pressure; unfortunately, this does not provide an unequivocal identification of the diffusion mechanism. On the other hand, the positive dependence on oxygen partial pressure found in San Carlos olivine precludes a vacancy mechanism for all the charge neutrality conditions considered by Stocker and Smyth (1977). Suggestions regarding the oxygen diffusion mechanism include a simple interstitial mechanism (Houlier et al. 1988), an interstitial mechanism where the diffusing species has a charge of −1 (Gérard and Jaoul 1989), a coupled counter-vacancy mechanism (Ryerson et al. 1989) or diffusion via cooperative motion of O3 and O2 ions (Brodholt 1997). No experimental methods to discriminate between these mechanisms have been proposed. While analysis of San Carlos olivine provides an experimentally accessible route to study the oxygen-diffusion mechanism, it is far from clear that the results are applicable to any other olivine sample, be it natural or synthetic. The diffusion mechanism may well depend on the concentration of other point defects (e.g. iron or hydrogen) in the sample and in order to understand oxygen diffusion under mantle conditions a range of different olivine samples should be studied.

Due in part to the extreme difficulty in conducting experiments of defect properties in crystalline solids, robust computational methods have been utilized to study defects. Olivine has often been investigated by these methods at various levels of theory and by a number of authors. Wright and Catlow (1994) used classical atomistic techniques to study the incorporation of water into the forsterite lattice. A similar approach was used by Jaoul et al. (1995) in order to study magnesium diffusion and by Richmond and Brodholt (2000) to study the incorporation of iron into forsterite. Ab initio electronic structure methods based on density functional theory have also been used. In the static limit (i.e. neglecting all vibrational energy) the generalized gradient approximation was used with a plane wave basis set to describe a charged cell containing ionic (Brodholt 1997) and protonated defects (Brodholt and Refson 2000).

Recently a combined atomistic–electronic structure method was used to examine hydrogen defects in forsterite (Braithwaite et al. 2002; 2003). This method exploits the strengths of the electronic structure and classical methods in unison. It bypasses possible artefacts caused by introducing a periodically repeating net charge within a super cell that can present difficulties in electronic structure methods and the limitations of the pair-potential technique that may inadequately describe the detailed structure of the defect. This is achieved by embedding an electronic structure description of the defect and its immediate surroundings in a deformable and polarizable atomistic model of the perfect solid. Although the embedded cluster technique is an extremely powerful method for the investigation of point defects, it is computationally time-consuming and therefore not well suited to a comprehensive study of the numerous possible diffusion pathways. However, we note that, in future, the embedding techniques could be used to refine the most important results presented within this paper.

The aim of the present work is to apply atomistic computational methods with a well-validated classical potential model to the problem of oxygen diffusion in olivine. Firstly, we will exploit the inherent atomic resolution of the method to systematically calculate the activation energy of diffusion by a number of well-defined possible competing mechanisms in forsterite. This allows us to predict the most favourable diffusion mechanism in a perfect forsterite crystal. We then examine the effect of iron and hydrogen on oxygen diffusion and attempt to understand the importance of such defects in natural olivine.

Method

We have systematically calculated the activation energy for diffusion by the simple vacancy hopping and interstitial mechanisms parallel to all three crystallographic axes. For each mechanism we break diffusion down into a series of "hops" between adjacent sites. Each hop is associated with a migration energy barrier. We limit ourselves to the vacancy and interstitial mechanisms in order to limit the number of hops to be considered. By making a series of hops, the diffusing ion may cross the unit cell. Under the assumption that consecutive hops are uncorrelated, the maximum migration energy required to achieve movement in a particular direction is the activation energy for diffusion in that direction. It is often possible for the ion to diffuse by more than one pathway across the cell; in these cases, the activation energy is the lowest activation energy of these routes. The mechanism with the lowest activation energy will be the dominant mechanism for diffusion. The activation energy found by this method assumes that there is no energetic cost associated with forming the diffusing defect. This is equivalent to assuming that the diffusing defect is present in the crystal because it compensates for the presence of charged impurities. Diffusion under these conditions is described as extrinsic. At high temperature the dominant contribution to the population of diffusing defects may be entropic. Diffusion is then termed intrinsic and the activation energy consists of two contributions, the formation energy of the diffusing defect and the height of the migration energy barrier. In materials containing ions with variable valance, a third diffusion regime is possible: transition-metal extrinsic diffusion (Chakraborty 1997) or constrained extrinsic diffusion (Jaoul et al. 1995). The diffusing defects arise in response to a change in the internal or external chemical potential. The activation energy for diffusion in this regime must include a contribution for the induced redox process.

In order to obtain the migration energies for each hop, we calculate the defect energies of a number of point defects and defect clusters in the static limit. The defects correspond to diffusing

species in their minimum energy configuration and in the activated state (the maximum energy configuration on the minimum energy pathway between two points). The migration energy is found by subtracting the energy of the initial, minimum-energy, state from that of the activated state. All energies are calculated using atomistic simulation techniques and the Mott–Littleton method implemented within the GULP code (Gale 1997).

Well-tested potential parameters (Catlow 1977b; Sanders et al. 1984; Lewis and Catlow 1985) were used to model forsterite and fayalite. Additionally, a simple model was used to describe the presence of OH^- defects (Schröder et al. 1992). The model is therefore based on an ionic description of the interatomic interactions with pair potentials described by formal ionic charges combined with a short-range Buckingham potential of the form:

$$V_{ij} = A_{ij} \exp\left(\frac{-r_{ij}}{\rho_{ij}}\right) - C_{ij} r_{ij}^{-6} \quad (3)$$

used to describe oxygen–oxygen and cation–oxygen interactions. This is supplemented by a harmonic three-body bond-bending interaction to provide the rigidity required to accurately model semicovalent SiO_4 tetrahedra. The polarization of oxygen is described using the shell model of Dick and Overhauser (1958). In this model, the charge of the ion is distributed between a negatively charged shell (notionally with no mass) and a positively charged core that interact only via a harmonic potential. Interactions between ions include core–core, core–shell and shell–shell Columbic interactions and short-range interactions that operate only between shells. The formal charges in the model probably overemphasize the ionic nature of olivine. This means that Columbic interactions are likely to be too large, which in turn causes features on the model potential energy surface to be overexpressed when compared to the real potential energy surface. We therefore expect the model to provide an upper bound on the migration energies calculated using it. However, errors arising from this are expected to be systematic and not to affect comparisons between competing mechanisms or diffusion pathways.

O–H bonds are described using a Coulomb-subtracted Morse potential of the form:

$$V_r = D(1 - \exp[-\alpha(r - r_0])^2 \ , \quad (4)$$

with parameters fitted to experimental data by Schröder et al. (1992). These potentials use fractional charges for the O and the H in the OH^- ion, but the hydroxyl has a formal charge of −1. In this description, hydrogen bonding is not directly represented (although the Buckingham potential contains an interionic attraction between non-bonded hydrogen and oxygen ions). Errors associated with the hydroxyl defects are therefore likely to be larger than the errors associated with the ionic model of olivine. The parameters of the potential model are given in Table 1. These parameters, derived empirically from experimental data for simple binary oxides (supplemented by quantum-mechanical data for the oxygen–oxygen interactions), have been successfully used for the modelling of the bulk (e.g. Price et al. 1987; Catlow and Price 1990) and defect (e.g. Wright and Catlow 1994; Jaoul et al. 1995; Richmond and Brodholt 2000) properties of forsterite and of a wide range of other silicates.

The energy of point defects and defect clusters is calculated using a method first suggested by Mott and Littleton (1938), implemented within GULP. In this method, a region around the defect (region I) is relaxed to an energy minimum using an interatomic potential. Region I is surrounded by a deformable portion of crystal that extends to infinity (region II). If the deformations in region II can be represented by a harmonic approximation, then the energy change induced by introducing the defect can be calculated from only the region I and region I–region II energy, i.e. the self-energy of region II need not be calculated explicitly. The problem of calculating the defect energy of such a model has been addressed by, for example, Norgett (1974) and is reviewed by Catlow and Mackrodt (1982). Following convergence tests, we truncated region I at a radius of 10 Å from the defect. Using the Mott–Littleton method means that the calculations are all performed on infinite model crystals with one isolated defect.

Table 1 Parameters of the potential model used in this study. Sources and equations are given in the text. The pair potentials are truncated beyond 10 Å

Charges (units of electronic charge)			Core–shell spring constant eV Å^{-2}
Ions	Core	Shell	
Mg	2.0		
Fe^{2+}	2.0		
Fe^{3+}	3.0		
Si	4.0		
O^{2-}	0.848190	−2.848190	74.92038
$O^{1.4-}$	−1.4260		
H	0.4260		
Buckingham potential	A (eV)	ρ (Å)	C (eV × Å^6)
Si–O^{2-}	1283.90734	0.32052	10.66158
Si–$O^{1.4-}$	983.556	0.32052	10.66158
O^{2-}–O^{2-}	22764.0	0.149	27.88
O^{2-}–$O^{1.4-}$	22764.0	0.149	27.88
$O^{1.4-}$–$O^{1.4-}$	22764.0	0.149	27.88
H–O^{2-}	311.97	0.25	0.0
H–$O^{1.4-}$	311.97	0.25	0.0
Mg–O^{2-}	1428.5	0.29453	0.0
Mg–$O^{1.4-}$	1060.5	0.29453	0.0
Fe^{2+}–O^{2-}	1207.6	0.3084	0.0
Fe^{3+}–O^{2-}	1102.4	0.3299	0.0
Morse (Coulomb-subtracted)	D (eV)	α (Å^{-1})	r_0 (Å)
H–$O^{1.4-}$	7.0525	2.1986	0.94285
Harmonic three-body	k (eV × rad^{-2})	θ_0 (degrees)	
O^{2-}–Si–O^{2-}	2.09724	109.47	
$O^{1.4-}$–Si–O^{2-}	2.09724	109.47	
$O^{1.4-}$–Si–$O^{1.4-}$	2.09724	109.47	

Minimum-energy configurations are found using standard quasi-Newtonian methods. The activated state is found utilizing a transition-state search algorithm based on the rational function optimization (RFO) procedure described by Banerjee et al. (1985) and implemented within GULP. This method is capable of locating saddle points on an energy surface from an arbitrary starting point. The saddle point found by the RFO method will correspond to the relevant transition state only if the initial defect geometry is close to the true transition state for the hop of interest. This is because the energy surface will contain a large number of saddle points for alternative hops and, possibly, for hops between intermediate states along the migration pathway. In order to ensure that the relevant saddle point was found, an initial survey of the energy surface was carried out via the technique of adiabatic mapping. This technique involves fixing the diffusing ion in a series of positions on a three-dimensional grid between the initial and final positions, and minimizing the energy of the rest of the structure. A trial transition structure is selected from this grid and used as an initial configuration for the RFO transition-state search.

We note that a problem was encountered when searching for the structure of the transition state that was found to originate from the shell model representation of the oxygen ion. This model allows the positively charged oxygen core to be displaced from the negatively charged oxygen shell in order to simulate the polarizability of the O^{2-} ion. As the ion moves away from its ideal minimum-energy site, it experiences an increasing polarization and, in regions where the anion is in an activated state, the electronic deformation of the ion may have strong multipolar components. These are inadequately represented by the dipolar shell model. This deficiency is often manifested within potential models like that outlined above by an excessive polarization of the ion; the shell may move too far and become disassociated from its core, resulting in a dramatic, unphysical, decrease in defect energy. This problem is similar to that described by Wojcik and Hermansson (1998) and is overcome by adding a large k_4 term that varies with the core–shell separation distance raised to the fourth power; this severely penalizes large separations. This term is removed once a trial transition state is found and the energies reported below do not include such a term.

Results

Perfect lattice and defect energies given by the model described above are presented in Table 2. The defects energies mark minima on the potential energy surface that are the start and end point for each hop; they are the reference energy used to calculate the height of the energy barrier. The results also enable a comparison of the performance of our atomistic model with that of higher-level treatments and allow us to consider diffusion outside of the extrinsic domain when corrections for the formation of the diffusing defect need to be made.

The results presented in Table 2 are in excellent agreement with previous work using the same potential model; this includes work that utilized the supercell approach (Richmond and Brodholt 2000) as well as the Mott–Littleton method used here (Wright and Catlow 1994; Jaoul et al. 1995). An additional test of the accuracy of these defect energetics is comparable with the results of electronic structure calculations. In general, we note good agreement with such calculations, in particular the defect formation energies calculated by Braithwaite et al. (2002) are in excellent agreement with our own values. Discrepancies between results obtained using the potential model and different electronic structure methods have been noted by Braithwaite et al. (2003) and Brodholt (1997). The sources of these differences are not clear but are the subject of our ongoing studies.

The broad agreement between electronic structure studies and our results for stable defects suggests that the potential model used in this study is appropriate for the description of defects in forsterite. This gives us confidence that the potential model will give qualitatively correct activation energies and the relative energetics are sufficiently accurate to be used in the interpretation of experimental data.

Table 2 Perfect lattice, reaction and defect energies for a range of possible defects in forsterite. Defects are described using Kröger–Vink defect notation and include vacancies in all three oxygen positions and oxygen interstitial ions occupying both free octahedral sites. Defect energies are with respect to the perfect forsterite lattice and the ion at infinity (which is defined so as to have zero potential energy). Lattice energies are for the reaction to bring together one formula unit of infinitely separated ions to form an infinite lattice and the reaction energies are to break the bond of a gas phase oxygen molecule, to add two electrons to a neutral gas-phase oxygen monoatom and to remove the electron from a gas-phase iron II ion, respectively

Defect	Defect energy (eV)
$V_{O1}^{\bullet\bullet}$	27.97
$V_{O2}^{\bullet\bullet}$	25.20
$V_{O3}^{\bullet\bullet}$	24.54
V''_{Mg1}	24.48
V''_{Mg2}	26.40
V''''_{Si}	100.81
$O''_{I(1)}$	−14.37
$O''_{I(2)}$	−16.11
$Fe^{\times}_{Mg1}$	1.08
$Fe^{\times}_{Mg2}$	0.97
$Fe^{\bullet}_{Mg1}$	−22.55
$Fe^{\bullet}_{Mg2}$	−23.24
$OH^{\bullet}_{O1}$	18.05
$OH^{\bullet}_{O2}$	16.87
$OH^{\bullet}_{O3}$	16.57
$OH'_{I(1)}$	−0.37
$OH'_{I(2)}$	−3.51
$[OH_{O1}V_{O2}]^{\bullet\bullet\bullet}$	44.66
$[OH_{O1}V_{O3}]^{\bullet\bullet\bullet}$	43.41
$[OH_{O2}V_{O1}]^{\bullet\bullet\bullet}$	46.09
$[OH_{O2}V_{O3}]^{\bullet\bullet\bullet}$	42.61
$[OH_{O3}V_{O1}]^{\bullet\bullet\bullet}$	43.07
$[OH_{O3}V_{O2}]^{\bullet\bullet\bullet}$	41.76
$[OH_{O3}V_{O3}]^{\bullet\bullet\bullet}$	42.74
Lattice	**Lattice energy (eV)**
Mg_2SiO_4 (forsterite)	−849.94
Fe_2SiO_4 (fayalite)	−844.49
MgO (periclase)	−41.31
Fe_2O_3 (hematite)	−124.83
Reaction	**Energy (eV)**
E_{OD}	5.19[a]
E_{A2}	6.80[b]
$E_{Fe(I3)}$	30.65[a]

[a] From the CRC handbook
[b] From Catlow (1977a)

Defects on the oxygen sublattice

In order to understand oxygen diffusion, it is essential to consider the distribution of defects on the oxygen sublattice. In this context it is useful to calculate the energy of partial (MgO) Schottky defect (Eq. 5) and the equivalent energy required to form an oxygen Frenkel defect (Eq. 6) in forsterite. This corresponded to two ways of introducing intrinsic defects into the oxygen sublattice.

$$\mathrm{Mg}_{\mathrm{Mg}}^{\times} + \mathrm{O}_{\mathrm{O3}}^{\times} \rightarrow V''_{\mathrm{Mg}} + V_{\mathrm{O3}}^{\bullet\bullet} + \mathrm{MgO}$$

$$E(\mathrm{MgO-Schottky}) = E\left(V''_{\mathrm{Mg}}\right) + E\left(V_{\mathrm{O3}}^{\bullet\bullet}\right) + U_{\mathrm{MgO}} = 7.71\,\mathrm{eV} \quad (5)$$

$$\mathrm{O}_{\mathrm{O3}}^{\times} \rightarrow \mathrm{O}''_{\mathrm{I(2)}} + V_{\mathrm{O3}}^{\bullet\bullet}$$

$$E(\mathrm{O-Frenkel}) = E\left(O''_{\mathrm{I(2)}}\right) + E\left(V_{\mathrm{O3}}^{\bullet\bullet}\right) = 8.43\,\mathrm{eV}\ . \quad (6)$$

As the Schottky energy is lower than the Frenkel energy, Schottky defects will predominate. Despite the small difference in energies, entropic considerations mean that we would not expect to find intrinsic oxygen interstitials in forsterite at any temperature of interest. However, at high oxygen partial pressure, oxygen interstitials may form due to the presence of impurities. For example, this may be mediated by the oxidation of iron II to iron III or the incorporation of iron III into the forsterite lattice. A plausible reaction for this process is:

$$2\mathrm{Fe}_{\mathrm{Mg}}^{\times} + \frac{1}{2}\mathrm{O}_{2(\mathrm{g})} \rightarrow 2\mathrm{Fe}_{\mathrm{Mg}}^{\bullet} + \mathrm{O}''_{\mathrm{I}}$$

$$E = 2E\left(\mathrm{Fe}_{\mathrm{Mg2}}^{\bullet}\right) - 2E\left(\mathrm{Fe}_{\mathrm{Mg2}}^{\times}\right) + 2E_{\mathrm{Fe(I3)}} + E\left(\mathrm{O}''_{\mathrm{I(2)}}\right) + 1/2E_{\mathrm{OD}} + E_{\mathrm{A2}} = 6.17\,\mathrm{eV}, \quad (7)$$

where E_{OD} is the dissociation energy of a oxygen molecule, E_{A2} is the sum of the first and second electron affinities of oxygen and $E_{\mathrm{Fe(I3)}}$ is the third ionization energy of iron. The values of these energies are taken from literature sources reported in Table 2. This reaction is similar in character to those recently considered by Tsai and Diekmann (2002), although these authors explicitly chose not to consider the presence of defects in the oxygen sublattice, in order to simplify their analysis. We, however, include the mechanism as a plausible route to the introduction of mobile oxygen defects. The oxygen interstitials formed by this process, or intrinsic oxygen vacancies, may diffuse.

Vacancy mechanism

One additional result of particular note is the large difference (at least 0.66 eV) between the energy required to form vacancies on the three symmetry-inequivalent oxygen sites. This was previously reported by Brodholt (1997) and was used to argue that almost all oxygen vacancies are to be found on the O3 site. In fact, at the melting temperature where this effect is smallest, Brodholt finds that less than 1 in 1000 oxygen vacancies will be on sites other than O3. This leads to a considerable simplification when considering the vacancy migration mechanism as we only need consider four hops between O3 sites rather than the 15 symmetry inequivalent hops between adjacent oxygen sites in the HCP sublattice. These four hops are shown in Fig. 2. Three of these hops are between adjacent O3 sites in the sublattice, the fourth (hop C) is a two-stage hop through interstitial I1. Two of the three simple hops (A and D) are hops between different SiO_4 tetrahedra, hop A resulting in a movement along [100] and [010] and hop B having a component only along [001]. Hop C is the hop between O3 sites belonging to the same SiO_4 unit.

Inspection of Fig. 2 gives the possible routes that a diffusing O3 vacancy may take to cross the unit cell in each direction. Diffusion parallel to [100] is only possible by repeated occurrences of hop A alternating with hop B. In either case for diffusion parallel to [100] the (extrinsic) activation energy will equal the migration energy of hop A. Diffusion parallel to [010] can be achieved by repeated occurrences of hop A, B and either hop C or D (the activation energy may be equal to the migration energy associated with any of these hops). Diffusion parallel to [001] requires either hops C and D, C and A, or D and A.

The migration energy calculated for each hop is reported in table 3. In each case diffusion will be rate-limited by hop A. This gives an extrinsic activation energy of 119 kJ mol^{-1} independent of the direction of diffusion.

As the energy of the activated state for hop A is higher than the energy minimum corresponding to a vacancy on the O2 site it is possible that there is a pathway that involves diffusion through the O2 site. Such a pathway was suggested by Brodholt (1997). In order to test this possibility we have calculated the migration energy for hops from O3 to O1 and O2 sites within the same SiO_4 tetrahedral unit. The energies of the activated states corresponding to these hops are 28.001 eV for the O3 to O1 hop and 27.159 eV for the

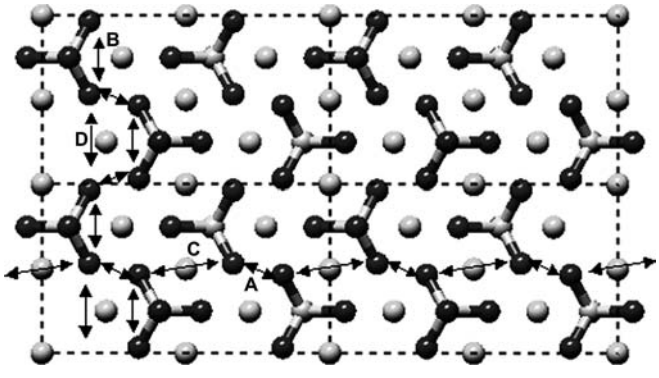

Fig. 2 Looking down [100] to four unit cells showing the possible routes for diffusion along [010] and [001] and all four hops (A–D, see text for details) assuming a vacancy mechanism where only O3 vacancies are involved. *Species* are shown as in Fig. 1

Table 3 Migration energies for vacancy and interstitial diffusion hops. *Hops A–D* are between O3 sites and *hops E–I* are for interstitial diffusion. *Hops E and F* are between adjacent I2 sites, *hops G–H* are from I2 to I1 sites and *hops G′–H′* are from I1 to I2 sites. The approximate hop distances are for straight lines measured in the perfect, undistorted, forsterite lattice

Hop	Approximate hop distance (Å)	Defect energy of initial state (eV)	Defect energy of activated state (eV)	Migration energy (eV)
A	3.0	24.54	25.765	1.23
B	2.6	24.54	25.260	0.72
C	3.4	24.54	25.223	0.69
D	3.3	24.54	31.270	6.73
E	3.0	−16.11	−14.942	0.97
F	3.0	−16.11	−15.144	1.17
G	3.5	−16.11	−13.542	2.57
G′		−14.37		0.83
H	3.3	−16.11	−14.265	1.85
H′		−14.37		0.11
I	3.4	−16.11	−13.177	2.93
I′		−14.37		1.19

O3 to O2 hop (hop distances are 2.8 and 2.5 Å, respectively). Therefore, the O3 to O3 hopping mechanism via hop A is the most energetically favourable.

Interstitial mechanism

For the interstitial migration mechanism we are not able to automatically eliminate hops using the assumption of defects occurring only on I2 sites, as was possible for the vacancy mechanism using the assumption of defects occurring only on O3 sites, as this would preclude diffusion along [010] by the interstitial mechanism. Instead, we assume that the unfavourable I1 sites are temporarily occupied by the diffusing ion. Although the activated state for hops from the I1 to the I2 site will be the same as for hops from the I2 to the I1 site, the energy of the initial configuration will be different. This means that the migration energy for the two types of hop will also be different. Hops involving interstitials are outlined in Fig. 3. Hops E and F are between adjacent I2 sites. Hops G, H and I are from I2 to I1 sites and G′, H′ and I′ are from I1 to I2 sites through the same activated state. Hops G, G′, H and H′ involve diffusion parallel to all three axes. The majority of movement achieved by hops I and I′ is made up of components along [010] and [001] directions.

Figure 3 shows the possible routes for interstitial diffusion across the unit cell. Diffusion parallel to [100] requires hop E and F, H and I′ or H′ and I. Diffusion parallel to [010] requires hop I, H or G and I′, H′ or G′. Diffusion parallel to [001] requires hop I, H or G and I′, H′ or G′, or hop E, or hop F. The calculated migration energies for these hops are presented in Table 3. These results give an extrinsic activation energy parallel to [100] of 113 kJ mol^{-1} rate limited by hop F. Diffusion parallel to [010] is rate-controlled by hop H with an activation energy of 178 kJ mol^{-1} and parallel to [001] the diffusion is controlled by hop E with an activation energy of 94 kJ mol^{-1}.

The effect of hydrogen and iron

In natural olivine, the oxygen-diffusion mechanism may be modified by the presence of iron in solid solution or by

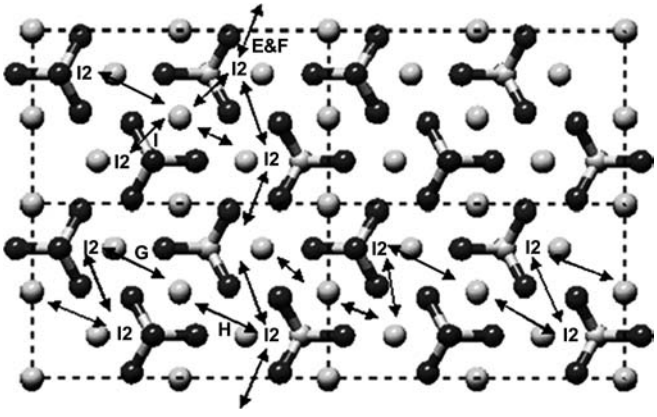

Fig. 3 Looking down [100] to four unit cells showing the possible routes for diffusion along [010] and [001] and all five hops (E–I, see text) assuming an interstitial mechanism where I2 sites are preferred over I1 sites. *Species* are shown as in Fig. 1. Only interstitial position I2 is shown for clarity

point defects, including those formed by the incorporation of water into the lattice. When iron replaces magnesium in the unit cell, the potential energy surface will be modified. There is also the possibility of redox reactions, where Fe^{2+} ions are oxidized to form Fe^{3+} ions. A key effect of such redox chemistry is likely to be enhancement of oxygen solubility in iron-bearing olivine when compared to pure forsterite, as suggested by Eq. (7). This could in turn lead to the extrinsic diffusion of oxygen interstitials. It has been shown by theory and experiment (e.g. Wright and Catlow 1994; Rossman 1996) that water will tend to dissociate and form OH^- point defects. If these defects diffuse more quickly than oxygen, oxygen diffusion may occur by the migration of these OH^- ions rather than by the migration of oxygen ions.

The magnitude of the effect of divalent iron in solid solution on the potential energy surface traversed by diffusing oxygen ions has been considered by calculating the lattice energy and defect energies for the initial state and transition state for hop A in pure fayalite. These are −842.23, 24.00 and 25.41 eV, respectively. The extrinsic activation energy for vacancy diffusion is therefore increased to 1.41 eV (135 kJ mol^{-1}). We expect this effect to diminish as the iron concentration decreases. The most important effect of iron upon defect mobility,

especially at the low iron concentrations found in the mantle, is due to its ability to change oxidation state.

As a first stage in the assessment of possible OH^- diffusion, we have calculated the energy of a number of OH^- defects including hydrogen bound to the three inequivalent oxygen ions, bound to interstitial oxygen and associated with oxygen ions adjacent to oxygen vacancies (Table 2). We then calculate the binding energy between OH^- occupying oxygen sites and oxygen vacancies:

$$\mathrm{OH}^{\bullet}_{\mathrm{O3}} + V^{\bullet\bullet}_{\mathrm{O3}} \rightarrow [\mathrm{OH}_{\mathrm{O3}} V_{\mathrm{O2}}]^{\bullet\bullet\bullet}$$

$$E(\mathrm{bind}) = E[(\mathrm{OH}_{\mathrm{O3}} V_{\mathrm{O2}})^{\bullet\bullet\bullet}] - \left[E\left(\mathrm{OH}^{\bullet}_{\mathrm{O3}}\right) + E\left(V^{\bullet\bullet}_{\mathrm{O3}}\right)\right] = 0.65\,\mathrm{eV}\ , \quad (8)$$

and the enthalpy of the reaction that results in an OH moving into an interstitial position, displacing the interstitial oxygen into the resulting vacancy:

$$\mathrm{OH}^{\bullet}_{\mathrm{O3}} + \mathrm{O}''_{\mathrm{I(2)}} \rightarrow \mathrm{O}^{\times}_{\mathrm{O3}} + \mathrm{OH}'_{\mathrm{I(2)}}$$

$$E = E\left(\mathrm{OH}'_{\mathrm{I(2)}}\right) - \left[E\left(\mathrm{OH}^{\bullet}_{\mathrm{O3}}\right) + E\left(\mathrm{O}''_{\mathrm{I(2)}}\right)\right] = -3.97\,\mathrm{eV}. \quad (9)$$

Equation (8) shows that there is a thermodynamic driving force that acts to separate hydrogen ions bound to lattice oxygen from oxygen vacancies (this value is for a dilute system and gives an upper bound for real systems). This is due to electrostatic repulsion between the two defects with effective positive charge. The implication is that the presence of hydrogen in the olivine lattice will not affect the rate of oxygen diffusion by the vacancy mechanism. Equation (9) indicates that, if oxygen interstitials and hydrogen already coexist, the hydrogen will tend to bind to the oxygen interstitial rather than any other lattice oxygen. If oxygen is diffusing by an interstitial mechanism, this may result in a change in diffusion rate. Based on the same hops that we considered for oxygen interstitial diffusion, we calculate the activation energy for interstitial OH^- diffusion. For hop E we calculate the energy of the activated state to be −1.17 eV giving an activation energy of 2.34 eV and for hop F we calculate the energy of the activated state to be −2.13 eV giving an activation energy of 1.37 eV (interstitial OH^- diffusion has a higher activation barrier than the diffusion of isolated oxygen ions). If both species (O^{2-} and OH^-) are present as interstitials, then oxygen diffusion will occur by the movement of oxygen interstitials rather than hydroxyl ions and the presence of hydrogen will not affect interstitial diffusion.

Discussion

The absolute accuracy of the energy determinations will, of course, depend on the performance of the potential model and especially its ability to describe defect structures and energetics. While the energy of stable defects calculated using this potential model is in fair agreement with available electronic structure calculations, we are not aware of any such studies that have attempted to compute the activated state geometry or the defect energy associated with the formation of interstitial oxygen. A critical test of the potential model would be to perform electronic structure calculations on our predicted activated state and compare the energy with that predicted by the potential model. This is a focus of our current investigations.

By breaking diffusion down into a series of hops, evaluating the migration energy for these hops and then calculating the activation energy for diffusion in each direction we have made some assumptions regarding the diffusion mechanism. The principal assumption is that between each hop the defect has time to reequilibrate so that each hop is independent of the next. The methodology also limits the mechanisms that can be studied. In essence, before the activated state can be found, the exact sequence of atomic movements of the proposed mechanism must be written down. This is possible when only one or two atoms move but if cooperative motion occurs the number of possible "hops" (each involving the movement of several ions) increases dramatically and it rapidly becomes unfeasible to consider all permutations. A method that is not subject to these limitations is molecular dynamics. In principle, in a long molecular dynamics simulation diffusion could be observed directly. However, even at high temperature, the extremely long simulation time required to observe the rare (less than one per ns) diffusion events requires very substantial amounts of computer time and a highly stable potential model.

The results indicate that, of the mechanisms considered, vacancy diffusion should be the dominant oxygen diffusion mechanism in pure forsterite. However, the extrinsic activation energies calculated above are clearly not comparable to the activation energies determined by experiment. Given the high temperature of the experiments on synthetic forsterite, and the high degree of purity of the samples, we believe that it is probable that they sampled the intrinsic diffusion regime. The intrinsic activation energy can found by adding the fraction of the defect formation (e.g. Schottky or Frenkel) energy required to form the diffusing species to the extrinsic activation energy. As Schottky defects will be the predominant intrinsic oxygen defect at high temperature, we therefore add 3.86 eV to the extrinsic activation energy to give an intrinsic activation energy 5.09 eV (492 kJ mol^{-1}). This energy is higher than all experimentally measured values. Reasonable explanations for this discrepancy include the fact that in the real crystals used in experiment, there will be a population of other defects (point, line and planar in nature) that will interact with the diffusing defect; using the Mott–Littleton method we do not attempt to treat these interactions. Additionally, the experimental values for the activation energy may, at the lowest temperatures, include data points which sampled the extrinsic regime. The credibility of this argument is enhanced when one

considers that in the experimental study that yields the largest activation energy (Ando et al. 1981; Oishi and Ando 1984) was conducted at, and sampled, the highest temperatures (and does not include temperatures below 1400 °C). Finally, the potential model includes formal charges; this may result in the barrier height being overestimated.

The experimental evidence supports an interstitial mechanism in natural samples. In cases where oxygen vacancies have been replaced by interstitials, the model predicts an extrinsic activation energy of 113 and 94 kJ mol^{-1} parallel to [100] and [001] and a much larger activation energy (178 kJ mol^{-1}) parallel to [010]. To this migration energy we must add a term for the formation of the diffusing defect. If oxygen interstitials form via the reaction outlined in Eq. (7), then the energy to be added is 2.06 eV (197 kJ mol^{-1}, one third of the total energy of the reaction) giving activation energies of 310, 375 and 291 kJ mol^{-1} along [100], [010] and [001], respectively. This is in fair agreement with the available experimental data, possible reasons for the small error in activation energy are the same as those discussed above with reference to vacancy diffusion. The anisotropy in activation energy is significant and may provide a method to experimentally discriminate between vacancy and interstitial mechanisms where diffusion is not sensitive to the oxygen partial pressure (i.e. in pure forsterite). Using only the results from this study it is not possible to give any indication of the expected anisotropy in the diffusivity of oxygen, except to say that there need be none when the vacancy mechanism is operational and the interstitial mechanism certainly will express such anisotropy. For the vacancy mechanism, the details of any anisotropy in diffusivity will depend only on the preexponential factor and will not change with temperature but for the interstitial mechanism the anisotropy in diffusivity will obviously be temperature-dependent as well.

Conclusions

The first conclusion that can be drawn from this study is that in forsterite, oxygen diffusion will occur by the vacancy mechanism, as would be expected on simple geometrical grounds. The atomistic model predicts that in the intrinsic high-temperature domain the activation energy for this process will be 492 kJ mol^{-1} and will be isotropic. The latter point is in complete agreement with what is found experimentally. The overestimation of activation energy may be due to inaccuracies in the potential model's description of the activated state or may indicate that the experimental results show a mixture of intrinsic and extrinsic diffusion. A major and perhaps surprising conclusion, given that the deformation of olivine varies with hydrogen content and is believed to be controlled by point defect diffusion, is that oxygen diffusion is not affected by varying the hydrogen content of the sample. However, we note that Jaoul (1990) predicts that oxygen diffusion should not affect creep rate and that Dohmen et al. (2002) find that the activation energies of creep and silicon diffusion in olivine are identical.

Experiments on natural olivine (reviewed in the Introduction) have been used to preclude a vacancy mechanism. One possibility is that at high oxygen partial pressure oxygen interstitials may be formed, mediated in natural olivine by the oxidation of iron II to iron III. If interstitial oxygen ions diffuse the model predicts that diffusion will be strongly anisotropic and yields activation energies in fair agreement with those found experimentally.

It is enlightening to compare these conclusions with Fig. 14 of Ryerson et al. (1989). This figure shows an Arrhenius diagram of oxygen diffusion in San Carlos olivine with two oxygen buffers. Two important observations can be made on increasing oxygen partial pressure by changing the oxygen buffer: (1) the diffusivity increases, (2) the activation energy becomes anisotropic with a difference between diffusion parallel to [100] and [010] of 71 kJ mol^{-1}. We would suggest that this is because the diffusion mechanism changes from the vacancy mechanism to the interstitial mechanism with increasing oxygen partial pressure. The computed energy difference between diffusion parallel to [100] and [010] is 65 kJ mol^{-1}, remarkably similar to the experimental value. However, currently available experimental data is insufficient to confirm this, and our study provides an interesting hypothesis to be tested. An ideal test would be to measure the dependence of diffusion on oxygen fugacity at both low and high oxygen fugacity separately and to measure the activation energy along all three axes under both sets of conditions. Our results could be used to evaluate such data and could also be used to interpret the diffusion mechanism in iron free olivine.

Acknowledgements A.M.W. acknowledges the receipt of a studentship from the Engineering and Physical Sciences Research Council and K.W. thanks the Royal Society for a university research fellowship. We wish to thank O. Jaoul for fruitful discussions and R. Dohmen and an anonymous reviewer for interesting and useful comments.

References

Ando K, Kurokawa H, Oishi Y, Takei H (1981) Self-diffusion of oxygen in single-crystal forsterite. Commun Am Ceram Soc 64:C-30

Banerjee A, Adams N, Simons J, Shepard R (1985) Search for stationary points on surfaces. J Phys Chem 89:52–57

Braithwaite JS, Sushko PV, Wright K, Catlow CRA (2002) Hydrogen defects in forsterite: a test case for the embedded cluster method. J Chem Phys 116:2628–2635

Braithwaite JS, Wright K, Catlow CRA (2003) A theoretical study of the energetics and IR frequencies of hydroxyl defects in forsterite. J Geophys Res 108: 2284–2292

Brodholt JP (1997) Ab initio calculations on point defects in forsterite (Mg_2SiO_4) and implications for diffusion and creep. Am Miner 82:1049–1053

Brodholt JP, Refson K (2000) An ab initio study of hydrogen in forsterite and a possible mechanism for hydrolytic weakening. J Geophys Res 105:18977–18982

Catlow CRA (1977a) Oxygen incorporation in the alkaline earth fluorides. J Phys Chem Solids 38:1131–1136

Catlow CRA (1977b) Point-defect and electronic properties of uranium dioxide. Proc Roy Soc (A) 353:533–561

Catlow CRA, Mackrodt WC (1982) Theory of simulation methods for lattice and defect energy calculations in crystals. In: Catlow CRA, Mackrodt WC (eds) Computer simulations of solids. Lecture notes in physics. Springer, Berlin Heidelberg New York pp 3–20

Catlow CRA, Price GD (1990) Computer modelling of solid-state inorganic materials. Nature 347:243–247

Chakraborty S (1997) Rates and mechanisms of Fe–Mg interdiffusion in olivine at 980 °C–1300 °C. J Geophys Res 120: 12317—12331

Dick BG, Jr, Overhauser AW (1958) Theory of the dielectric constants of alkali halide crystals. Phys Rev 112:90–103

Dohmen R, Chakraborty S, Becker H-W (2002) Si and O diffusion in olivine and implications for characterizing plastic flow in the mantle. Geophys Res Lett 29:2030

Gale JD (1997) GULP: a computer program for the symmetry-adapted simulation of solids. J Chem Soc Faraday Trans 93:629–637

Gérard O, Jaoul O (1989) Oxygen diffusion in San Carlos olivine. J Geophys Res 94:4119–4128

Houlier B, Jaoul O, Abel F, Liebermann RC (1988) Oxygen and silicon self-diffusion in natural olivine. Phys Earth Planet Int 50:240–250

Jaoul O, (1990) Multicomponent diffusion and creep in olivine. J Geophys Res 95:17631–17642

Jaoul O, Froidevaux C, Durham WB, Michaut M (1980) Oxygen self-diffusion in forsterite: implications for the high-temperature creep mechanism. Earth Planet Sc Lett 47:391–397

Jaoul O, Houlier B, Abel F (1983) Study of ^{18}O diffusion in magnesium orthosilicate by nuclear microanalysis. J Geophys Res 88:613–642

Jaoul O, Bertran-Alvarez Y, Liebermann RC, Price GD (1995) Fe–Mg interdiffusion in olivine up to 9 GPa at $T = 600$–900 °C; experimental data and comparison with defect calculations. Phys Earth Planet Int 89:199–218

Lewis GV, Catlow CRA (1985) Potential models for ionic oxides. J Phys (C): Solid State Phys 18:1149–1161

Mott NF, Littleton MJ (1938) Conduction in polar crystals. I. Electrolytic conduction in solid salts. Trans Faraday Soc 34:485

Norgett MJ (1974) A general formulation of the problem of calculating the energies of lattice defects in ionic crystals. UK Atomic Energy Authority report number: AERE-R7650 pp 49

Oishi Y, Ando K (1984) Oxygen self-diffusion coefficient in single-crystal forsterite. In: Sunagawa I (eds) Materials science of the Earth's interior. Terra Scientific, Tokyo, pp 271–280

Price GD, Parker SC, Leslie M (1987) The lattice dynamics and thermodynamics of the Mg_2SiO_4 polymorphs. Phys Chem Miner 15:181–190

Reddy KPR, Oh SM, Major LD, Jr, Cooper AR (1980) Oxygen diffusion in forsterite. J Geophys Res 85:322–326

Richmond NC, Brodholt JP (2000) Incorporation of Fe^{3+} into forsterite and wadsleyite. Am Mineral 85:1155–1158

Rossman GR (1996) Studies of OH in nominally anhydrous minerals. Phys Chem Miner 23:299–304

Ryerson FJ, Durham WB, Cherniak DJ, Lanford WA (1989) Oxygen diffusion in olivine: effect of oxygen fugacity and implications for creep. J Geophys Res 94:4105–4118

Sanders MJ, Leslie M, Catlow CRA (1984) Interatomic potentials for SiO_2. J Chem Soc Chem Comm 19: 1271–1273

Schröder KP, Sauer J, Leslie M, Catlow CRA, Thomas JM (1992) Bridging hydroxyl groups in zeolitic catalysts: a computer simulation study. Chem Phys Lett 188:320–325

Sockel HG, Hallwig D (1977) Ermittlung kleiner Diffusionskoeffizienten mittels SIMS in oxydischen Verbindungen. Mikrochim Acta Suppl 7:95–107

Sockel HG, Hallwig D, Schachtner R (1980) Investigations of slow exchange processes at metal and oxide surfaces and interfaces using secondary ion mass spectrometry. Mat Sci Eng 42:59–64

Stocker RL, Smyth DM (1977) Effect of enstatite activity and oxygen partial pressure on the point-defect chemistry of olivine. Phys Earth Planet Int 16:145–156

Tsai T-L, Diekmann R (2002) Variation of the oxygen content and point defects in olivines, $(Fe_xMg_{1-x})_2SiO_4$, $0.2 < x < 1.0$. Phys Chem Miner 29:680–694

Wojcik MC, Hermansson K (1998) The problem of the detaching shells in the shell model potential for oxides. Chem Phys Lett 289:211–218

Wright K, Catlow CRA (1994) A computer simulation study of (OH) defects in olivine. Phys Chem Mins 20:515–518